



# Long-term spatiotemporal variation of drought patterns over the Greater Horn of Africa

Gebremedhin Gebremeskel Haile<sup>a,b,c</sup>, QiuHong Tang<sup>a,b,\*</sup>, Guoyong Leng<sup>a</sup>, Guoqiang Jia<sup>a</sup>, Jie Wang<sup>a</sup>, Diwen Cai<sup>a</sup>, Siao Sun<sup>a</sup>, Binod Baniya<sup>a</sup>, Qinghuan Zhang<sup>a</sup>

<sup>a</sup> Key Laboratory of Water Cycle and Related Land Surface Processes, Institute of Geographic Sciences and Natural Resources Research, Chinese Academy of Sciences, Beijing, China

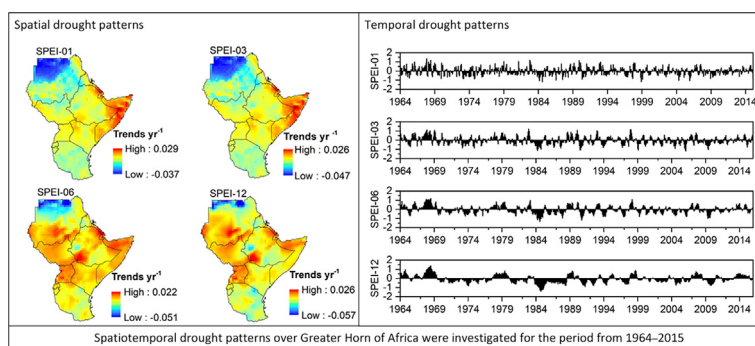
<sup>b</sup> University of Chinese Academy of Sciences, Beijing, China

<sup>c</sup> Tigray Agricultural Research Institute, Mekelle, Ethiopia

## HIGHLIGHTS

- Spatiotemporal drought patterns were investigated in the Greater Horn of Africa.
- Droughts showed an increasing annual trend during 1964–2015.
- Droughts in 1973–74, 1984–85, and 2010–11 were severe and intense.
- Droughts increased in winter, spring and summer but decrease in autumn season.
- Information on historical droughts is helpful to adapt and alleviate drought.

## GRAPHICAL ABSTRACT



## ARTICLE INFO

### Article history:

Received 31 May 2019

Received in revised form 27 September 2019

Accepted 29 October 2019

Available online 24 November 2019

Ouyang Wei

### Keywords:

Drought characteristics

Drought trends

Standardised Precipitation-Evapotranspiration Index

East Africa

## ABSTRACT

Understanding historical patterns of changes in drought is essential for drought adaptation and mitigation. While the negative impacts of drought in the Greater Horn of Africa (GHA) have attracted increasing attention, a comprehensive and long-term spatiotemporal assessment of drought is still lacking. Here, we provided a comprehensive spatiotemporal drought pattern analysis during the period of 1964–2015 over the GHA. The Standardised Precipitation-Evapotranspiration Index (SPEI) at various timescales (1 month (SPEI-01), 3 month (SPEI-03), 6 month (SPEI-06), and 12 month (SPEI-12)) was used to investigate drought patterns on a monthly, seasonal, and interannual basis. The results showed that despite regional differences, an overall increasing tendency of drought was observed across the GHA over the past 52 yr, with trends of change of  $-0.0017 \text{ yr}^{-1}$ ,  $-0.0036 \text{ yr}^{-1}$ ,  $-0.0031 \text{ yr}^{-1}$ , and  $-0.0023 \text{ yr}^{-1}$  for SPEI-01, SPEI-03, SPEI-06, and SPEI-12, respectively. Droughts were more frequent, persistent, and intense in Sudan and Tanzania, while more severe droughts were found in Somalia, Ethiopia, and Kenya. Droughts occurred frequently before the 1990 s, and then became intermittent with large-scale impacts occurred during 1973–1974, 1984–1985, and 2010–2011. A turning point was also detected in 1989, with the SPEI showing a statistically significant downward trend during 1964–1989 and a non-statistically significant downward trend from 1990 to 2015. Seasonally, droughts exhibited an increasing trend in winter, spring, and summer, but a decreasing trend in autumn. The research findings have significant implications for drought adaptation and mitigation strategies through identifying the hotspot regions across the GHA at various timescales. Area-specific efforts are required to alleviate environmental and societal vulnerabilities to drought events.

© 2019 Elsevier B.V. All rights reserved.

\* Corresponding author.

E-mail address: [tangqh@igsnrr.ac.cn](mailto:tangqh@igsnrr.ac.cn) (Q. Tang).

## 1. Introduction

Droughts can result in environmental and societal impacts globally. The United Nations listed drought as the “most far-reaching of all-natural disasters” on Earth (United Nations, 2014). Drought is often referred to as an elusive phenomenon with variable onset and termination, thereby making its management challenging (Bachmair et al., 2016). Droughts occur naturally (Mukherjee et al., 2018), but can be aggravated by various climatic and anthropogenic drivers (Mishra and Singh, 2010; Sheffield et al., 2012). As a result, an increasing trend of drought events has been observed at the global scale with substantial regional variations (Dai, 2011a; IPCC, 2013; He et al., 2016; Baniya et al., 2019). Sheffield and Wood (2008) claimed that long-term droughts have become three times more frequent globally. There is increasing evidence that the frequency and extent of droughts have become longer and more intense in the past few decades (Nicholson, 2017; Sivakumar et al., 2014), and will intensify in magnitude and severity worldwide within the context of global warming (IPCC, 2013; Sheffield and Wood, 2008). Thus, region-specific explorations of drought are critical for effective and efficient drought monitoring and adaptation strategies.

Droughts are common in the Greater Horn of Africa (GHA), which is where arid and semiarid climate systems are dominant (Sivakumar et al., 2014; Measho et al., 2019). In the GHA, drought frequency and duration have recently increased and become widespread (Ayana et al., 2016; Guha-Sapir et al., 2004; Nicholson, 2017). Droughts can last for two or more rainy seasons with severe socioeconomic consequences (Anderson et al., 2012). The environmental and socioeconomic impacts caused by droughts are manifested by a lack of water, pastures, energy, and food; famine; loss of livestock, life, and property; mass migration; and environmental refugees (Lyon and Dewitt, 2012; Tierney et al., 2015). Meanwhile, food security in less developed regions, which have also been experiencing increasing population growth, is often threatened by the deleterious consequences of droughts (Brown and Funk, 2008; Funk et al., 2008). The challenges facing sustainable water use and food production over the GHA are expected to persist in the future (Funk et al., 2015). Thus, enhancing the regional adaptation capacity is becoming crucial in the face of recurrent drought episodes over the GHA. Increased data availability from remote sensing products, reanalysis, and land surface models, along with gauged datasets, have greatly facilitated drought monitoring and management and have enabled a detailed investigation of droughts across the GHA (Agutu et al., 2017).

Even though there are serious droughts in the GHA, the long-term spatial variation and temporal evolution of drought patterns remain largely unexplored. As a result, appropriate early warning and drought adaptive strategies towards drought management have rarely been implemented in the region. The governments, stakeholders, and communities have mainly focused on crisis management (Sivakumar et al., 2014; Tadesse et al., 2008) rather than prediction and management of droughts ahead of their occurrence. In addition, long-term comprehensive studies focusing on drought occurrences in the past with future implications are lacking. To this end, there is a pressing need to investigate the long-term historical spatiotemporal patterns of droughts over the GHA. The quantification of drought events in time and space would have an invaluable use for society and the environment. In addition, it would allow for exploration of the long-term annual and seasonal drought trends. Spatiotemporal drought analysis is undertaken considering various drought characteristics, including drought duration, frequency, severity, and intensity (Mishra and Singh, 2010). Providing such detailed drought characteristic information to users is critical for

monitoring and management of droughts, as drought information is primarily used for drought forecasting and early warning ahead of its occurrence.

Drought is measured by drought indices of varying complexities, thereby leading to discrepancies in the quantification and interpretation of drought (IPCC, 2013). Thus, the selection of a drought index depends on the purpose of its development and the user's objective for drought analysis. In this study, the main objective was to explore the spatial variations and temporal evolutions of long-term drought patterns in the GHA. As droughts have been increasing under global warming in the GHA (Muller, 2014), an appropriate drought index should reflect the effects of global warming. Therefore, selection of a drought index that incorporates the effects of global warming conditions is necessary. In this study, we used the Standardised Precipitation-Evapotranspiration Index (SPEI; Vicente-Serrano et al., 2010a), which was designed to investigate the evolution of drought under global warming (Liu et al., 2016). Specifically, the SPEI has the ability to identify droughts induced by increasing atmospheric water demand via evapotranspiration (Adhyani et al., 2017). Notably, the SPEI has the advantage of representing different drought types, such as meteorological, agricultural, hydrological, and socioeconomic droughts (Chen and Sun, 2015). The SPEI has the combined advantages of the Palmer Drought Severity Index (PDSI; Palmer, 1965) and Standardised Precipitation Index (SPI; Mckee et al., 1993). Numerous studies have used the SPEI at various timescales to examine changes in drought under global warming (e.g. Chen and Sun, 2015; López-Moreno et al., 2013; Wang et al., 2018; Yu et al., 2014).

Understanding historical drought variations is vital for enhancing the resilience to future droughts. In addition, in order to establish a regional drought policy and strategy, the development of a comprehensive drought monitoring system is critical (Asong et al., 2018). Based on long-term historical drought information, the efficient early warning of drought onset, severity, persistence, and spatial extent enables drought risk alleviation ahead of its occurrence. For this reason, the study of long-term SPEI time series for efficient water resource management at the regional level is important. Thus, this study intended to investigate the spatial and temporal patterns of drought frequency, duration, and intensity focusing on long-term drought assessments over the GHA in the past 52 yr (1964–2015). The 1, 3, 6, and 12 month timescales were employed for constructing the drought index, which could be used to measure the impact of drought on various water resource needs (Mckee et al., 1993).

This paper is organised as follows. Following the introduction, Section 2 provides a description of the study area, data, methods, and drought index. Section 3 presents the detailed results of the spatial and temporal patterns of drought at seasonal and annual scales. Section 4 provides a discussion, followed by the conclusion in Section 5.

## 2. Materials and methods

### 2.1. Study area

The GHA and East Africa represent the same geographical area (Anyah and Semazzi, 2006; Haile et al., 2019; Nicholson, 2017). It comprises 11 countries, namely Djibouti, Eritrea, Ethiopia, Kenya, Somalia, South Sudan, Sudan, Tanzania, Rwanda, Burundi, and Uganda (Fig. 1). Geographically, GHA is located between 11.76°S and 23.15°N and 21.84°E and 51.42°E, with an estimated area of 6.22 million km<sup>2</sup>. The total population in the GHA is around 360 million. Most of the population resides in the East African highlands. A wide altitudinal range from 153 m below sea level (at Lake

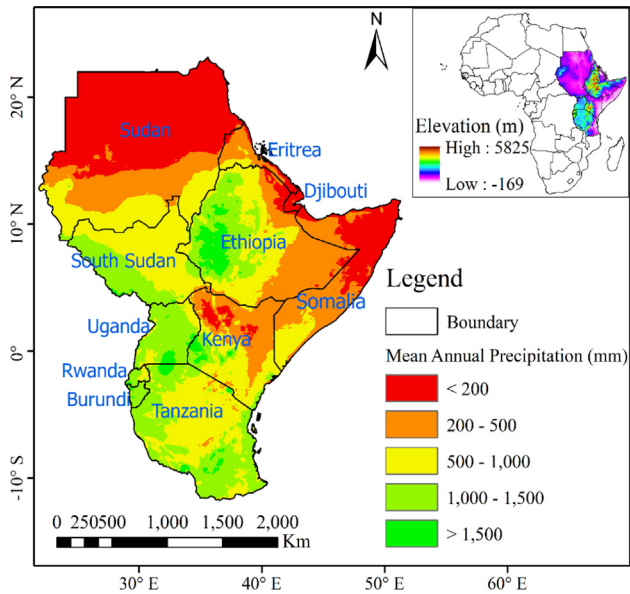


**Fig. 1.** Geographical location and mean annual precipitation of the Greater Horn of Africa.

Assal in Djibouti) to 5895 m above sea level (at Mt. Kilimanjaro in Tanzania) is found in the GHA (Camberlin, 2018). Moreover, the GHA is home to a number of large water bodies and wetlands across the Great East African Rift Valley region. The land cover is dominated by grasslands and shrublands, with scattered evergreen forests in southwestern parts of Ethiopia and other isolated patches in Kenya, Tanzania, and Uganda.

The GHA is a relatively dry area (Camberlin, 2018), with about 69% of the region classified as hyperarid, arid, and semiarid (UNDP/UNSO, 1997). The hyperarid and arid areas are inhabited by pastoralists (Ayana et al., 2016). Agriculture is the core of the GHA economy, which is characterised by low-income countries. This means that rainfall is key for social and economic development in the GHA. Much of the region is characterised by different rainfall seasons, i.e. boreal spring (March–May), boreal summer (July–September), and boreal autumn (October–December) (Nicholson, 2014). The GHA highlands, including Mt. Kenya, Mt. Kilimanjaro, the Ethiopian highlands, and some parts of Tanzania and Uganda, receive the greatest rainfall, whereas the arid and semiarid areas, such as eastern Somalia, the arid and semiarid lands region of Kenya, eastern Ethiopia, and Djibouti, receive much less rainfall (Nicholson, 2017). In addition, the annual rainfall is lower than 400 mm in large parts of Sudan, Djibouti, the Red Sea coast, Afar depression, and northern Somalia (Camberlin, 2018). The GHA region is also known for its variations in interannual rainfall owing to greater climate variability (Dinku et al., 2011; Funk et al., 2015; Schreck and Semazzi, 2004). The Intertropical Convergence Zone, El Niño Southern Oscillation, and sea surface temperature variations in the Indian and Pacific oceans are the main drivers of climate variability in the region (Lyon and Dewitt, 2012; Tierney et al., 2013).

## 2.2. Data and computational procedures

For this study, drought magnitude was quantified using the multi-scalar SPEI metric dataset (SPEIbase v.2.5) (<http://sac.csi.ces/spei/database.html>). This SPEI dataset was developed using the monthly gridded data of precipitation (P) and temperature (Vicente-Serrano et al. 2010b) of the Climatic Research Unit (CRU) TS3.24.01 dataset (Harris et al., 2014; New et al., 2000)

(<http://badc.nerc.ac.uk/data/cru/data/hrg/>). The principal sources of the monthly climate archives of the CRU TS3.24 dataset are the World Meteorological Organization and global meteorological stations ([http://hadobs.metoffice.com/crutem3/data/station\\_updates/](http://hadobs.metoffice.com/crutem3/data/station_updates/)) in collaboration with the US National Oceanographic and Atmospheric Administration (<http://www1.ncdc.noaa.gov/pub/data/mcdw/>) (Harris et al., 2014; New et al., 2000). Both the CRU TS3.24.01 and SPEIbase v.2.5 datasets were developed in pixels of  $0.5^\circ \times 0.5^\circ$  spatial resolution. The SPEI dataset is widely used as it is readily available for long periods and spans large areas. As a result, many studies have used the SPEI dataset for drought analyses at global and regional scales (e.g. Schwalm et al., 2017). The SPEI datasets were used to identify droughts from 1964 to 2015 in the GHA.

The SPEI dataset incorporates the effects of temperature on the water cycle via evapotranspiration (Wang et al., 2018), and is highly sensitive to changes in temperature within the context of global warming (Vicente-Serrano et al., 2010a). Specifically, the Penman-Monteith method (<http://www.fao.org/3/X0490E/x0490e06.htm>) (Allen et al., 1998) was employed to calculate the potential evapotranspiration (PET), based on which the probability distribution function of the difference between P and PET was derived. The difference between P and PET was used to measure the water surplus or deficit in a given time period (Chen and Sun, 2015). The log-logistic distribution was applied at 1, 3, 6, and 12 month timescales to facilitate both short and medium-term drought analysis. The SPEI was obtained by standardising and normalising the sequences of the probability distribution function. Details on the SPEI calculation procedures can be found in the study by Vicente-Serrano et al. (2010a).

## 2.3. Methods of drought analysis

Drought is measured by drought indices at various spatiotemporal levels. There are various drought indices that can be used on the basis of their characteristics and user needs. For reliable drought risk assessment and decision-making, a multivariate drought index is preferable over a single variable (e.g. P, soil moisture, or runoff)-dependent index (AghaKouchak, 2015; Hao and AghaKouchak, 2014). Thus, a drought index that combines multiple variables together should be used for more accurate drought monitoring.

The SPEI (Vicente-Serrano et al., 2010a) is a multi-scalar metric typically used for drought analysis and evaluation under a changing climate. The SPEI measures the difference between water supply (i.e. P) and demand (i.e. atmospheric water demand linked to temperature). For this study, the SPEI was used to investigate spatiotemporal patterns of drought considering the effects of temperature (Liu et al., 2016) over the drought-prone GHA. Here, the SPEI values were estimated at multiple timescales, namely 1 month (SPEI-01), 3 month (SPEI-03), 6 month (SPEI-06), and 12 month (SPEI-12). The SPEI-01 and SPEI-03 were used to identify short-term drought events, while the SPEI-06 and SPEI-12 were used for assessing long-term drought events (Asong et al., 2018). The SPEI at different timescales can reflect the imbalance of various water cycle components. For example, the SPEI-01 and SPEI-03 generally reflect meteorological and agricultural droughts, respectively, while the SPEI-06 to SPEI-12 are for hydrological drought analyses (Asong et al., 2018). The thresholds for defining each drought severity level are the same as those used for the SPI (Mckee et al., 1993).

### 2.3.1. Drought characteristics analysis procedures

Drought characteristics are mainly explained by different drought conditions, such as duration, frequency, severity, and intensity (Lee et al., 2017; Zhang et al., 2015). A widely used

probabilistic method, namely the theory of runs, has been used to understand the characteristics of drought (Yevjevich, 1967). In this study, the runs theory was applied using the SPEI time-series data to detect drought duration, frequency, and intensity in the GHA. Drought is identified when the SPEI value drops below the threshold value ( $-1$ ) (Schwalm et al., 2017; Xu et al., 2018). The higher negative values below  $-1$  indicate more severe drought relative to average long-term conditions. The more negative the SPEI, the more severe the drought, and vice versa (Spinoni et al., 2014; Xu et al., 2018). The negative SPEI values also indicate the lack of rain relative to the atmospheric water demand. Drought properties, including duration, frequency, and intensity, were determined for each drought event during the past 52 yr over the GHA.

**2.3.1.1. Drought duration.** Drought duration ( $D$ ) is the length of time (i.e. the number of months) between the onset and termination of drought (Mao et al., 2017; Spinoni et al., 2014). It is calculated by the sum of the durations for all drought events divided by the number of drought events, as follows (Xu et al., 2018; Eq. (1)):

$$D = \frac{\sum_{i=1}^n d_i}{n} \quad (1)$$

where  $d_i$  is the duration of the  $i$ th drought event in an area and  $n$  is the total number of drought events in the area.

**2.3.1.2. Drought frequency.** Drought frequency refers to the number of drought occurrences in a given time period (Yu et al., 2014). It is estimated as the ratio between the number of drought months and the total number of months in the time series (Spinoni et al., 2014; Wang et al., 2018; Eq. (2)).

$$F = \frac{n_m}{N_m} \times 100\% \quad (2)$$

where  $F$  is the drought frequency,  $n_m$  is the number of drought months, and  $N_m$  is the total number of months ( $52 \times 12 = 624$  months in this case).

**2.3.1.3. Drought intensity.** Another important parameter is drought intensity. Drought intensity measures drought severity according to its duration, which is useful for determining the strength of droughts (Zhang et al., 2015). It is the absolute value of the average of accumulated SPEI values during the drought events (Wang et al., 2018), which is given as Eq. (3). For each duration of the drought event, drought severity measures the cumulative deficit below the truncation level to quantify the drought intensity (Zhang et al., 2015). The estimation of drought intensity helps to detect how intensified droughts can lead to drying the environment.

$$I = \left| \frac{1}{n} \sum_{i=1}^n SPEI_i \right| \quad (3)$$

where  $I$  is the drought intensity,  $n$  is the number of drought occurrences, and  $SPEI_i$  is the accumulated SPEI value below the threshold for drought event  $i$ .

### 2.3.2. Drought trend analysis techniques

The non-parametric Mann-Kendall (MK) trend test (Kendall, 1955; Mann, 1945) was used to evaluate the trends of changes in drought in the GHA. The MK test can be used for inhomogeneous time series data and has low sensitivity to data that are not normally distributed. The MK test was used to detect the existence of temporal trends in the SPEI time series using the  $Z_{mk}$  test statistic. Details of the  $Z_{mk}$  test statistic calculation can be found in the studies by Mann (1945) and Kendall (1955). In our study, the significance of the trends was tested at the  $\alpha = 0.05$  significance level. The null hypothesis of no trend was rejected if  $|Z_{mk}| > 1.96$ .

The change over time (i.e. slope) was used to calculate the magnitude of the trends in the SPEI time series data (Eq. (4)). The slope estimated by the regression model indicated the mean temporal change in the SPEI, with negative and positive slopes indicating increasing and decreasing trends of the SPEI values, respectively. The slopes of annual and seasonal drought trends were also computed for analysis. The overall variation of drought trends in each pixel and time length was estimated during 1964–2015. Equation (4) was used to detect the changing pattern of droughts in each pixel.

$$\text{Slope} = \frac{n \times \sum_{i=1}^n (i \times SPEI_i) - (\sum_{i=1}^n i) \times (\sum_{i=1}^n SPEI_i)}{n \times \sum_{i=1}^n i^2 - (\sum_{i=1}^n i)^2} \quad (4)$$

where  $i$  is the series number of the year,  $n$  is the length of the time series, and  $SPEI_i$  represents the drought occurring in the  $i$ th year.

Moreover, when the time series SPEI data lacked a significantly increasing or decreasing trend, a segment-wise turning point analysis was conducted (Chen et al., 2014). This technique was used to detect the potential turning points in the SPEI time series.

## 3. Results

### 3.1. Spatial patterns of drought

#### 3.1.1. Spatial distribution of drought duration and frequency

Drought duration and frequency are important properties of droughts. Fig. 2a shows the mean duration of droughts at various timescales over the GHA during 1964–2015. Overall, the north of the GHA in Sudan and the east in Somalia have experienced longer drought durations than those of other regions (Fig. 2a), thereby posing significant challenges for their agriculture, ecosystems, and society (Chen and Sun, 2015). The Ethiopian highlands, Tanzania, Rwanda, Burundi, and parts of Kenya have shorter drought durations (Fig. 2a). Thus, the spatial distribution of drought duration during the period of 1964–2015 allowed us to detect the drought-prone countries in the GHA.

The average drought durations in the GHA were 1.46, 2.32, 3.59, and 7.60 month for the SPEI-01, SPEI-03, SPEI-06, and SPEI-12, respectively. Drought duration tended to increase with the SPEI timescale, although similar patterns were observed among the timescales (Fig. 2a). That is, droughts identified based on the SPEI-06 and SPEI-12 persisted longer than those based on the SPEI-1 and SPEI-3. Drought duration increased with the timescale, and droughts at the SPEI-12 or larger timescales tended to persist much longer (Mpelasoka et al., 2018). Generally, large drought duration values indicated the existence of persistent short-term drought events with a longer length, while smaller values indicated the frequent but intermittent occurrence of short drought events. Short-term droughts may pose serious threats to agriculture, whereas long-term droughts affect the hydrological cycle (Rhee and Cho, 2015; Steinemann et al., 2015).

Drought frequency showed distinct spatial patterns over the GHA during the past 52 yr (Fig. 2b), with high frequencies observed in Sudan, parts of Ethiopia, Eritrea, South Sudan, and Tanzania irrespective of the SPEI timescale used. In contrast, countries such as Rwanda, Burundi, parts of Uganda, Somalia, and Ethiopia have experienced a relatively small number of droughts. For the GHA as a whole, the average drought frequency of 19.57%, 19.54%, 19.31%, and 19.48% was detected based on the SPEI-01, SPEI-03, SPEI-06, and SPEI-12, respectively. Across the timescales, non-statistically significant spatial variations in drought frequency were observed at the regional scale. However, large interannual variability of drought frequency was found during the past five decades. Generally, drought frequency at short timescales

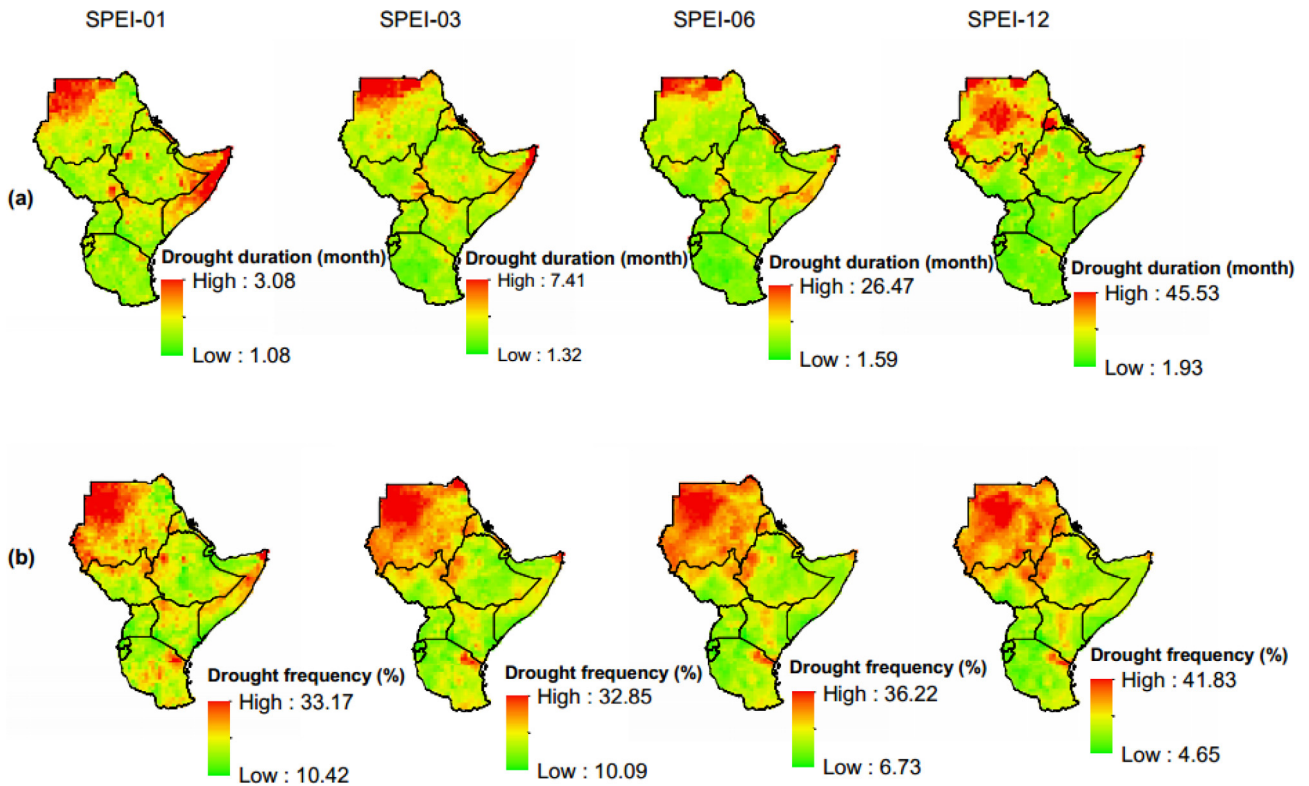


Fig. 2. Long-term spatial variations of (a) drought duration and (b) drought frequency in the Greater Horn of Africa during 1964–2015.

(SPEI-01 and SPEI-03) fluctuated more than that at relatively longer timescales (SPEI-06 and SPEI-12) (Liu et al., 2016).

### 3.1.2. Spatial distribution of drought intensity

Drought intensity showed a consistent spatial distribution over the GHA during 1964–2015 among the timescales (Fig. 3). Large intensity was observed in Sudan, parts of Eritrea, Uganda, and Tanzania, and near the borders of South Sudan and Ethiopia; low intensity was observed in major parts of Ethiopia, Djibouti, and Tanzania. The average drought intensity for the GHA was 0.072, 0.100, 0.130, and 0.180 based on the SPEI-01, SPEI-03, SPEI-06, and SPEI-12, respectively. These results suggested that as there

was a substantial increase in drought intensity with the timescale, and differences in the timescales led to significant differences in drought intensity. This indicated that a consistent seasonal and interannual spatial variation of drought intensity across the GHA needs to be considered corresponding to the timescale employed. Therefore, drought adaptation and mitigation measures might depend on the results of the timescale considered, which is higher at seasonal and interannual scales.

### 3.1.3. Spatial distribution of drought trends

Fig. 4 shows the spatial distribution of drought trends across the GHA. Decreasing SPEI trends were found in the northern part of the

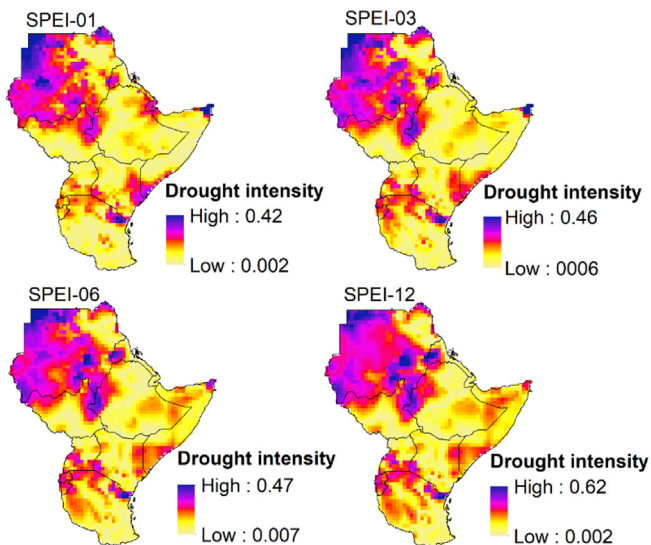


Fig. 3. Long-term spatial variations of drought intensity in the Greater Horn of Africa during 1964–2015.

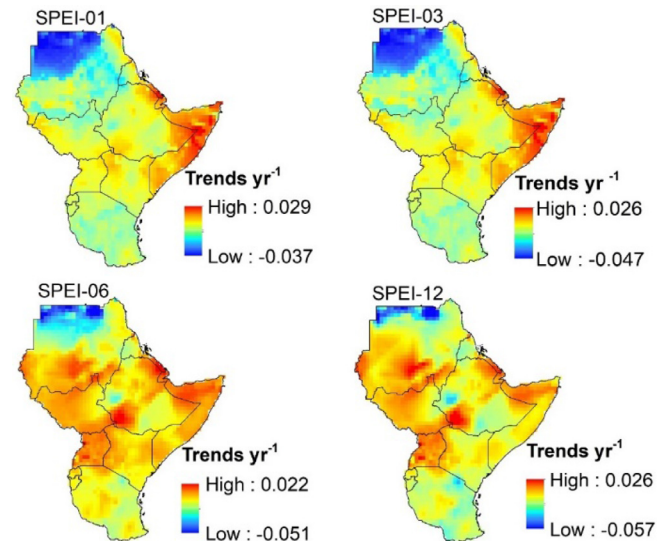


Fig. 4. Long-term spatial drought trend variations in the Greater Horn of Africa during 1964–2015.

GHA, whereas increasing trends were observed in the eastern areas of the GHA. Notably, the more negative the SPEI value, the greater the drought. The increasing SPEI trends (changes per year) were especially evident in Somalia, Tanzania, eastern Eritrea, western Ethiopia, and Uganda at all timescales, thereby indicating a decrease in drought, while trends of small change were found in parts of northern Sudan, Tanzania, and south Ethiopia, which was where recurrent drought events have occurred since the 1980s. In a similar manner, Mpelasoka et al. (2018) indicated that the drought areal extent has shown increasing trends. The greater the magnitude of drought, especially in Sudan, is a reflection of its arid climate system. The northern part of the GHA, particularly in the arid zone of northern Sudan, is visibly dry (Camberlin, 2018). This can lead to persistent drought over dry areas, while its P was low. This could be a clear indicator of the aforementioned drought characteristic parameters. Thus, a brief understanding of the inherently dry areas is vital. The mean values of drought trends were  $-0.0017 \text{ yr}^{-1}$ ,  $-0.0036 \text{ yr}^{-1}$ ,  $-0.0031 \text{ yr}^{-1}$ , and  $-0.0023 \text{ yr}^{-1}$  for SPEI-01, SPEI-03, SPEI-06, and SPEI-12, respectively. Despite the non-evident difference in the spatial pattern of drought trends shown in Fig. 4, the overall decreasing SPEI trends shown in Fig. 7 indicated that drought has increased in the GHA. The central parts of the GHA tended to have similar trends to those found in between the eastern and northern parts.

### 3.2. Temporal drought variations

#### 3.2.1. Long-term yearly drought variations

Fig. 5 shows the variation of the yearly SPEI of various time series in the GHA during 1964–2015. The drought increased through much of the SPEI time series. It was evident that drought had increased, especially after 1980 (Fig. 5). Droughts were more severe during 1980–2000 than those during other periods. Droughts increasingly occurred during the study period with various magnitudes. For example, the 1984–1985 severe drought in Ethiopia and Sudan was induced by persistent rainfall shortages during the rainy season (Degefu and Bewket, 2015), which resulted in migration and death.

In the GHA, historical droughts have negatively affected societies and environments, as confirmed by the famine during 2002–2003 (in Ethiopia) and 2010–2011 (in the Horn of Africa) (Ayana et al., 2016; Tadesse et al., 2008). In particular, Somalia, Ethiopia, and Kenya have been severely affected by drought episodes over the GHA (AghaKouchak, 2015; Agutu et al., 2017).

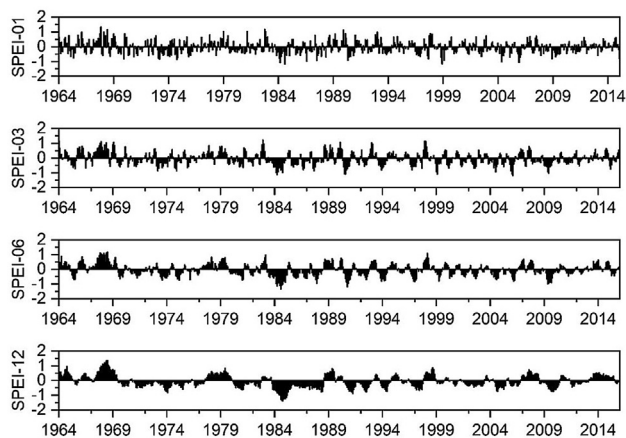


Fig. 5. Long-term temporal patterns of drought in the Greater Horn of Africa for the 1 month Standardised Precipitation-Evapotranspiration Index (SPEI-01), SPEI-03, SPEI-06, and SPEI-12 during 1964–2015.

#### 3.2.2. Long-term monthly drought variations

Fig. 6 shows the monthly time series of average SPEI values during 1964–2015 for each of the timescales. The patterns of monthly drought variation showed similar trends among the four timescales, but the drought extent and magnitude increased with the timescale. As indicated in Fig. 5, despite inconsistent patterns, a decreasing trend was found for all the SPEI timescales during 1964–2015. Notably, during 1968, almost all months experienced water excess, while a water deficit was reported for all months in 1973–1974, 1984–1985, and 2010–2011. The monthly SPEI captured the wetting trend in 1968 and the drying trend in 1985 well.

During 1964–1980, fewer drought events were recorded in the GHA, especially for the months of May–July. During 1981–2000, drought increased in both magnitude and extent, especially for August–October during 1984–1987 and June–October during 1989–1991, which had considerable impacts on the environment and society.

Since 2000, country-level drought has occurred in one or more months at all the timescales (Table 1). The 2002–2003 Ethiopia drought affected more than 14 million people with severe consequences (AghaKouchak, 2015; Funk, 2009; Muller, 2014; Nicholson, 2017). The 2010–2011 drought in the GHA (particularly in the Horn of Africa region), such as in Somalia, Ethiopia, and Kenya, was the worst drought in 60 yr (AghaKouchak, 2015; Nicholson, 2017). It was evident that few droughts occurred in the October–December months (Fig. 5) owing to the increase in rainfall in the “short rains” season (e.g. Lyon and Vigaud, 2017).

### 3.3. Annual and seasonal drought trends

#### 3.3.1. Annual drought trends

The temporal trends based on the MK test and slope are given in Fig. 7 for each timescale during 1964–2015. The MK trend analysis revealed that drought has increased over the past 52 yr. The *P* values for each timescale (SPEI-01, SPEI-03, SPEI-06, and SPEI-12) are given in Fig. 7, and the corresponding annual trend slope values were  $-0.002$ ,  $-0.004$ ,  $-0.002$ , and  $-0.002$ , respectively. The fluctuating downward trend in Fig. 7 indicates that the SPEI time series increased in the region, but was non-statistically significant. Similar results were found by Mpelasoka et al. (2018), who reported that the long-term probability of annual drought occurrences has shown non-statistically significant trends across the GHA.

The SPEI time series data were further analysed to detect the potential turning point (Chen et al., 2014). As shown in Fig. 8, a turning point was detected in 1989 with a statistically significant downward trend during 1964–1989 and non-statistically significant downward trend during 1990–2015 (Fig. 8). These results suggested that although drought showed an overall increasing trend, there were decadal fluctuations. These differences in trends were likely due to changes in climatic and environmental conditions in the past three decades. In addition, the oceanic, seasonal, and rainfall characteristics might have also contributed to the differences.

Multi-year drought fluctuations were evident with different patterns and trends among different areas (Figs. 5 and 8). These were consistent with the results of Mpelasoka et al. (2018), who indicated that the long-term probability of annual drought occurrences ranges from 20% to 30%. Moreover, significant drought events occurred in different years. The increasing drought trends indicated that the number of drought years increased in the GHA, thereby causing damage to agriculture and water resource facilities (Yu et al., 2014). The negative SPEI values for all timescales suggested that drying events might have been amplified over the GHA (Figs. 7 and 8). The most severe drought years were 1973–1974, 1984–1985, and 2010–2011, which resulted in larger impacts on the environment and society (Haile et al., 2019), especially in Somalia, Ethiopia, Kenya, and Sudan.

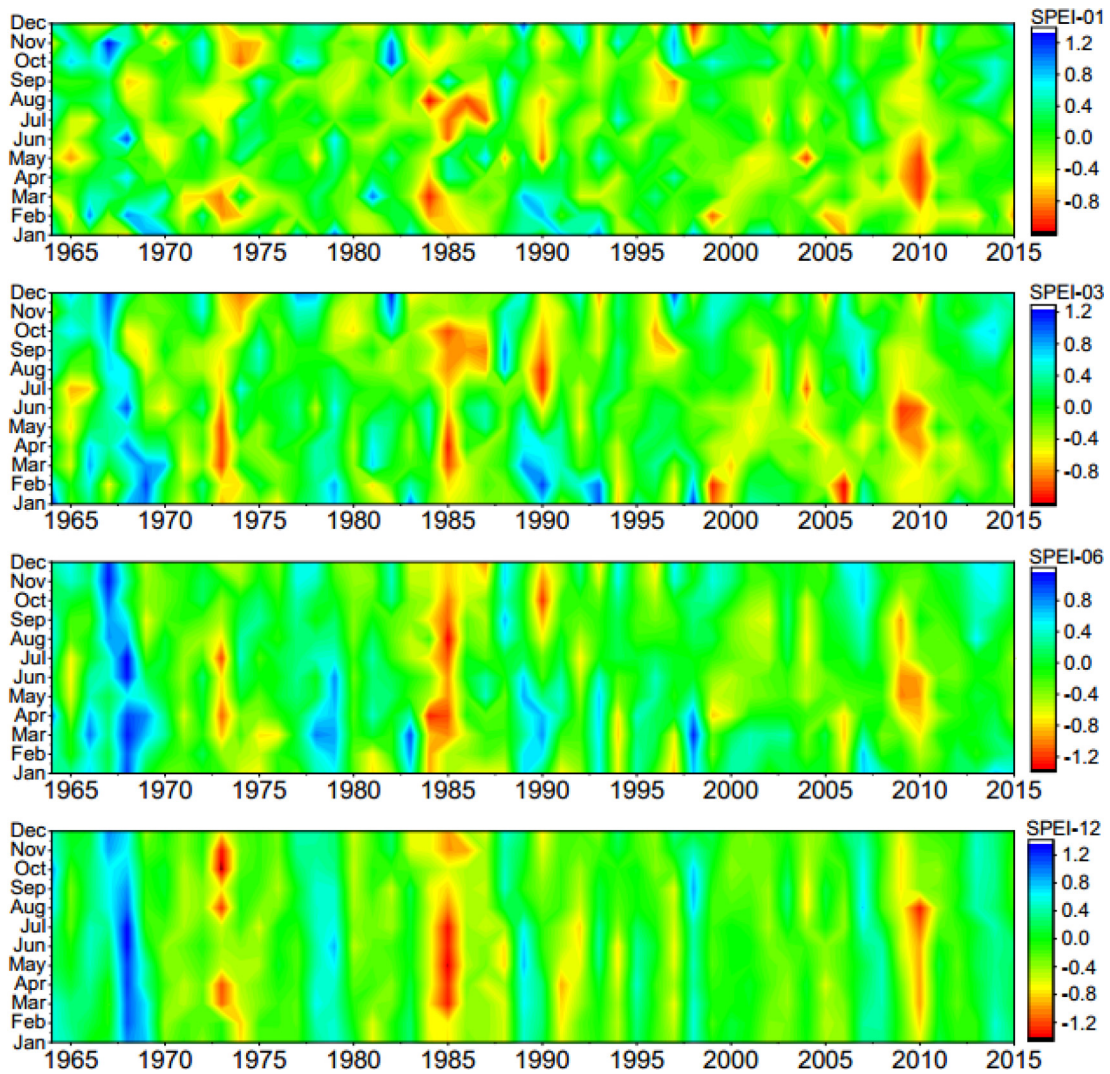


Fig. 6. Patterns of monthly responses to drought at different temporal scales during 1964–2015.

Table 1

Summary of drought events recorded in 1964–2015 in the Emergency Events Database (EM-DAT, 2018) and the literature (e.g. Guha-Sapir et al., 2004; Masih et al., 2014).

Countries in East Africa	Years' range 1964–1970	1971–1980	1981–1990	1991–2000	2001–2010	2011–2015
Burundi	–	–	–	1999	2003, 2005, 2008, 2009, 2010	–
Djibouti	–	1980	1983, 1988	1996, 1999	2005, 2007, 2008, 2010	–
Eritrea	–	–	–	1993, 1999	2008	–
Ethiopia	1965, 1969	1973	1984, 1987, 1989	1997, 1998, 1999	2003, 2005, 2008, 2009	2012, 2015
Kenya	1965	1971, 1979	1983	1991, 1994, 1996, 1999	2004, 2005, 2008, 2010	2012, 2014
Rwanda	–	1976	1984, 1989	1996, 1999	2003	–
Somalia	1965, 1969	1973, 1980	1983, 1987, 1988	1999	2004, 2005, 2008, 2010	2012, 2014
South Sudan	–	–	–	–	2010	–
Sudan	–	–	1980, 1983, 1987, 1990	1991, 1996, 1999	2009	2012, 2015
Tanzania	1967	1977	1984, 1988, 1990	1996	2003, 2004, 2006	2011
Uganda	1967	1979	1987, 1998	1999	2002, 2005, 2008, 2010	–

Note: non-drought periods are represented by an em dash (–).

### 3.3.2. Seasonal drought trend patterns

The temporal variation of the SPEI at each timescale is given in Figs. 9 and 10 and Supplementary S1 and S2 for spring, autumn, winter, and summer, respectively, for the period of 1964–2015. There were variations in the drought trends among the different seasons. Generally, winter, autumn, and summer droughts exhibited similar increasing trends. Droughts showed an increasing

trend in spring, winter, and summer, but with significant differences in magnitude. For all timescales, the temporal trend of each season, except for autumn, showed a downward SPEI trend, thereby suggesting that drought was increasing.

During the winter season, a downward trend of the SPEI was found for all timescales except for the SPEI-06, thereby indicating that drought increased (Supplementary S1). The years with winter

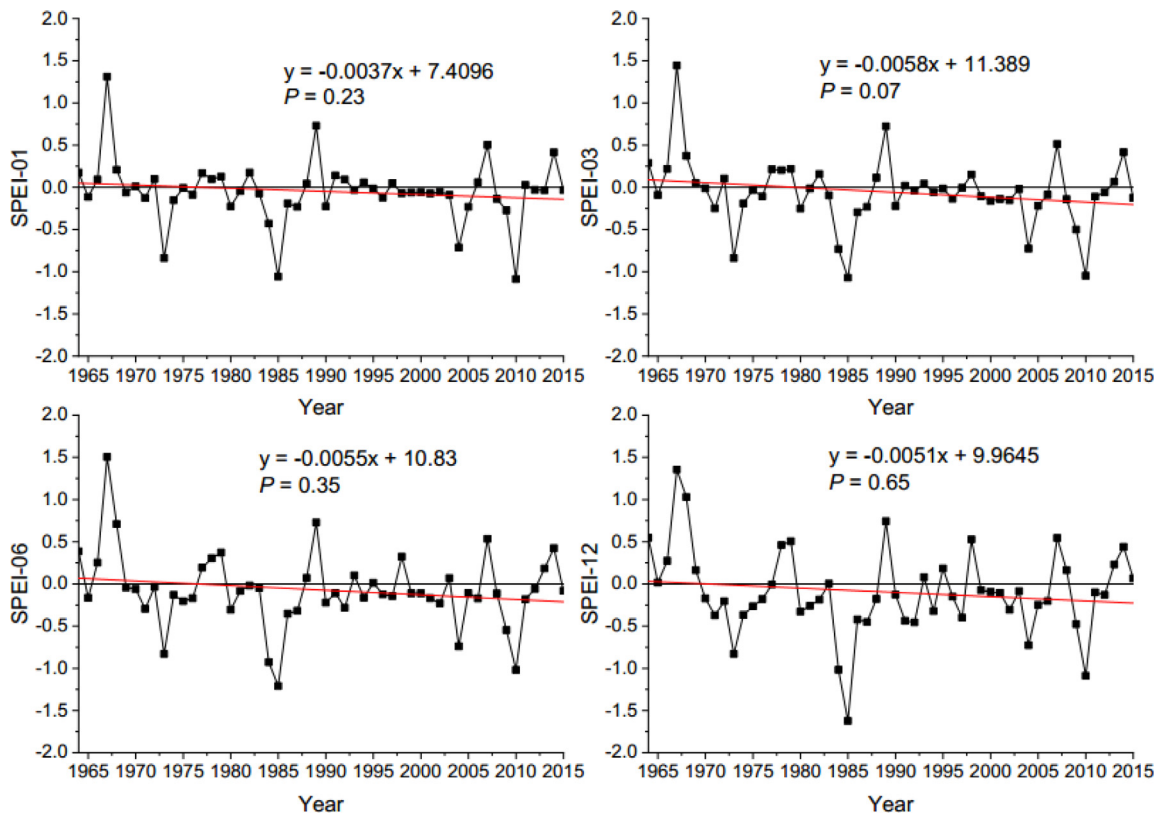


Fig. 7. Temporal variation of the annual Standardised Precipitation-Evapotranspiration Index (SPEI) in the Greater Horn of Africa at each timescale during 1964–2015.

SPEI values that dropped below the threshold were 1973–1974, 1984–1985, and 2010–2011, which were consistent with the results of previous reports (Lyon and Vigaud, 2017; Nicholson, 2017). These droughts have led to famine in the drought-vulnerable countries of the GHA. During the spring season, drought showed a significant downward trend ( $\alpha < 0.05$ ) (SPEI-03 and SPEI-06) and non-statistically significant downward trend (SPEI-01 and SPEI-12) (Fig. 9). Meanwhile, the spring season showed similar trends to those in winter (Supplementary S2). In the GHA, the spring season features “long rains”, and crops are mainly grown in this season (AghaKouchak, 2015; Nicholson, 2017). The occurrence of prolonged water shortages in the spring season would cause large-scale impacts in the region. Thus, early warning systems are necessary to prevent drought occurrence and its consequences.

During the summer season, the SPEI time series showed a decreasing trend, as indicated in the downward trends of the SPEI for all timescales (Supplementary data S2). However, the SPEI values during the summer did not show large variations compared with those of other seasons. The summer season is the main rainy season in the northern and northeastern parts of the GHA (Agutu et al., 2017).

Unlike that in other seasons, an upward trend was observed for the SPEI-01, SPEI-03, and SPEI-06 during autumn (Fig. 10). This indicated that meteorological and agricultural droughts decreased in the region. In the GHA, the autumn season is commonly called the “short rains” season (Haile et al., 2019). Previous studies showed that the short rains season’s rainfall has been increasing, and consequently the autumn drought has decreased during 1964–2015 (Agutu et al., 2017; Anderson et al., 2012).

Generally, the season-based drought trend analysis showed similarities in drought conditions, except for the autumn season. This suggested that drought mitigation strategies should be based on the specific season of interest. It is evident that as this study

covered a large geographical extent with variable climatological conditions, the results would be different when a specific region or country is considered in the GHA.

## 4. Discussion

### 4.1. Spatiotemporal drought characteristics

P and temperature variations have direct impacts on the occurrence of drought. It is known that droughts occur with below-normal P persisting for more than three consecutive months (Liu et al., 2016). Drought indices are used to measure how much P and temperature (in the form of PET) for a given period deviate from historical averages in time and space. Spatiotemporal drought investigation is of great importance for enhancing the resilience of drought-prone areas of the GHA. In this study, drought was characterised by its duration, frequency, intensity, and linear trends. The drought duration, frequency, and intensity explained the long-term spatiotemporal drought variations in the GHA. Considering various timescales of drought indicators is crucial for understanding the evolution of drought over the GHA. The timescales of the SPEI are also relevant for explaining the temporal and spatial drought variabilities. To this end, the mean annual droughts based on the SPEI values increased with the timescale (Steinemann et al., 2015). From the analysis of the SPEI timescales, drought mostly responded to longer SPEI timescales, which was consistent with the findings of Potopová et al. (2018) and Vicente-Serrano et al. (2012). This indicated that drought indicators at longer timescales (SPEI-06 and SPEI-12) are substantially more severe than those at shorter timescales. This could help to assess the multi-dimensional droughts of various timescales. Normally, meteorological drought can be represented by the SPEI-01, the SPEI-03 represents the agricultural drought conditions, and hydrological droughts are mostly represented by the SPEI-06 and SPEI-12

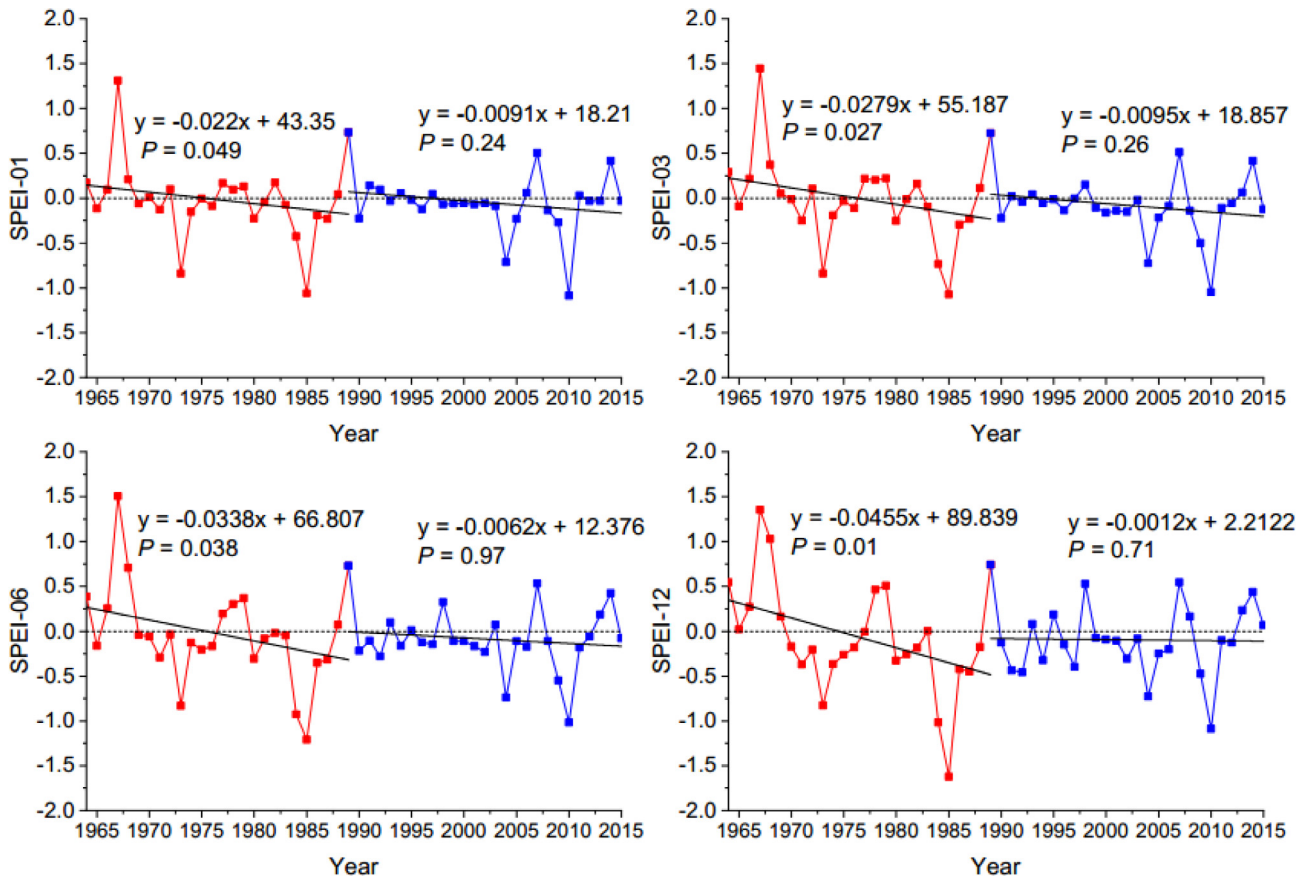


**Fig. 8.** Temporal variation of the annual Standardised Precipitation-Evapotranspiration Index (SPEI) over the Greater Horn of Africa for each timescale from 1964 to 2015. The red and blue lines indicate the time series data of the SPEI during 1964–1989 and 1990–2015, respectively. (For interpretation of the references to colour in this figure legend, the reader is referred to the web version of this article.)

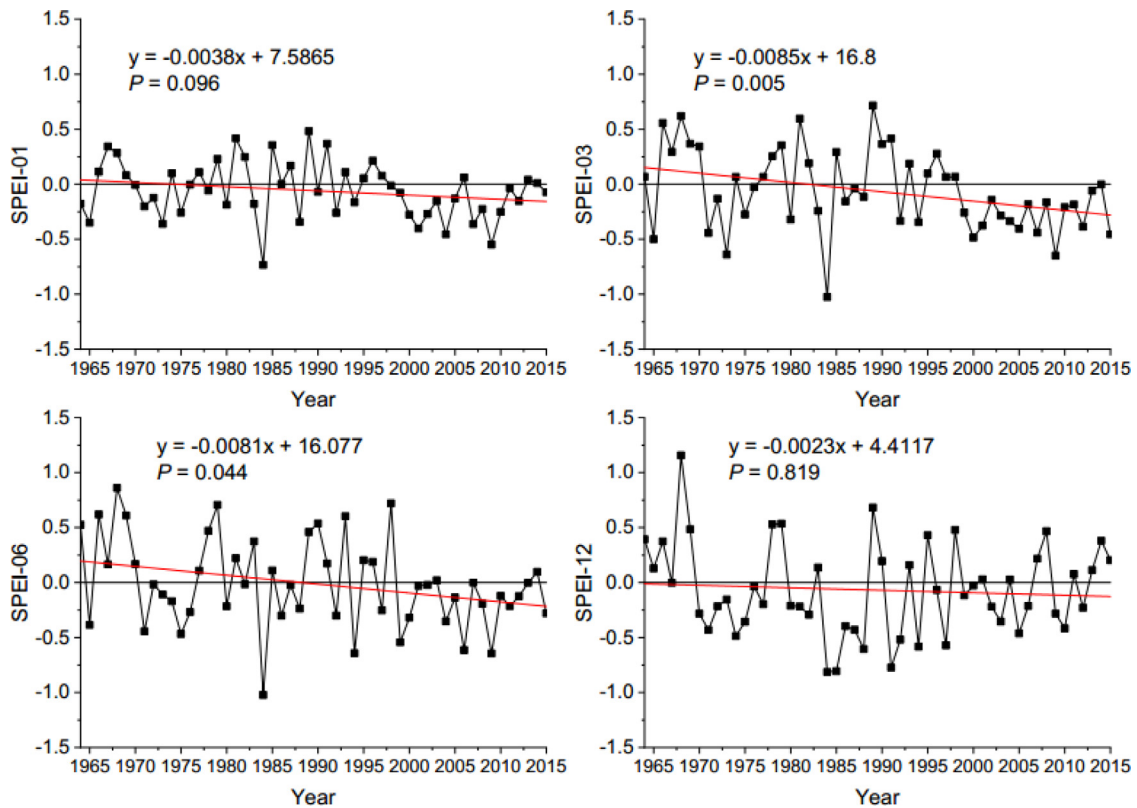


**Fig. 9.** Temporal Standardised Precipitation-Evapotranspiration Index (SPEI) variation of the spring season in the Greater Horn of Africa from 1964 to 2015.

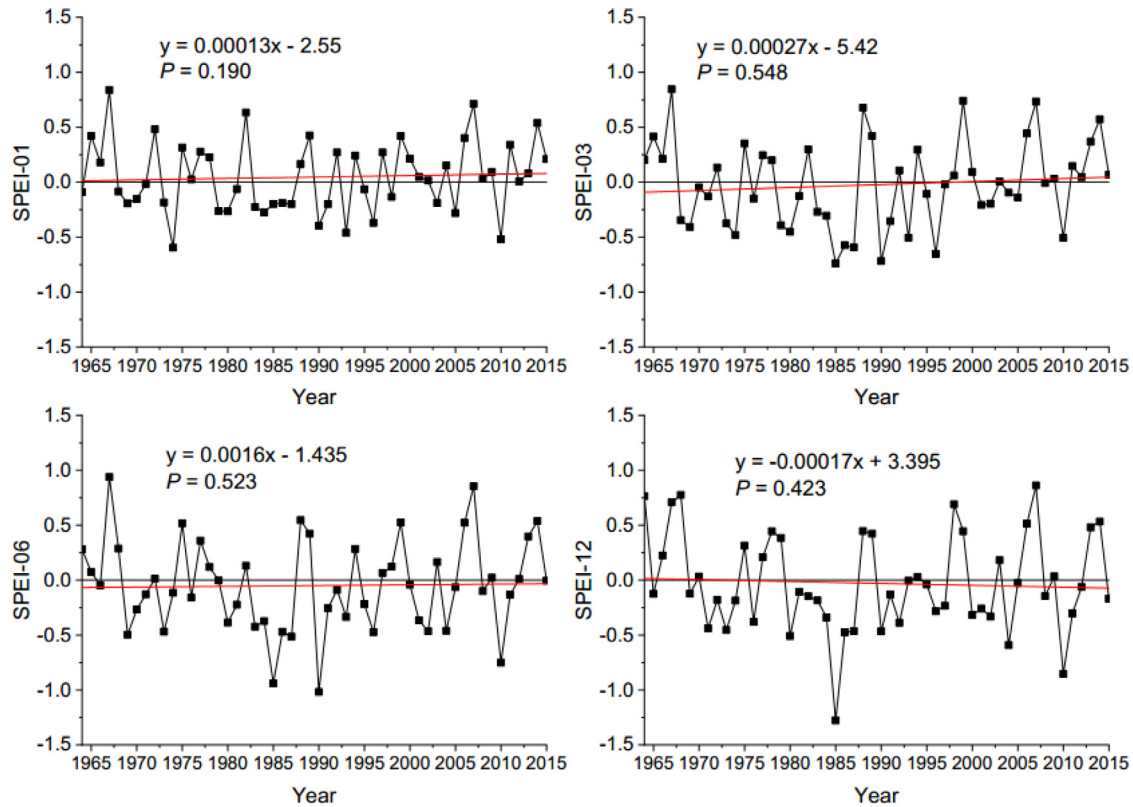


Fig. 10. Temporal Standardised Precipitation-Evapotranspiration Index (SPEI) variation of the autumn season in the Greater Horn of Africa from 1964 to 2015.

(Asong et al., 2018). These droughts have propagation behaviours from meteorological to agricultural and then hydrological droughts (Van Loon, 2015). When drought propagates to hydrological drought, it is difficult to recover within a short period. Similar results could also be obtained when using other drought indices. For instance, Ntale and Gan (2003) indicated that the SPI has been used for monitoring droughts in the GHA owing to its modest data requirements for any timescale.

Moreover, the drought characterising components, such as duration, frequency, and intensity, have been widely used in the literature (Spinoni et al., 2014; Xu et al., 2015; Yu et al., 2014; Zhan et al., 2016). These studies showed a significant drying trend and increasing drought patterns. Investigation of the spatiotemporal patterns of drought can help to better understand the mechanism and influencing factors of drought occurrence and evolution (Zhou et al., 2017). Generally, higher drought frequency and longer drought duration with higher intensity are distributed in Sudan and parts of Tanzania and South Sudan, while a higher magnitude of drought severity is found in Somalia, Ethiopia, and Kenya. These countries are characterised by arid and semiarid climate conditions with frequent occurrence of severe droughts (Zhou et al., 2017). The remaining GHA countries have also faced similar drought events of various magnitudes. Overall, the increase in drought frequency, duration, and severity was found to be significant in the GHA, and similar results were also found in the literature (e.g. Spinoni et al., 2014).

#### 4.2. Driving factors for drought occurrence and evolution

The main driving factors for the increased occurrence of drought in the GHA are natural climate variability and anthropogenic influences (Dinku et al., 2011; Funk et al., 2015; IPCC, 2013; Trenberth et al., 2014). The climate system over the GHA is inherently variable with complex topographies ranging from arid

lowlands to wetter highlands and coastal areas (Dinku et al., 2011; Funk et al., 2015; Schreck and Semazzi, 2004). The major climatic factor influencing droughts is the seasonal dynamics of tropical circulations expressed as the El Niño Southern Oscillation (Ogalo et al., 2008). The influence of El Niño (the warm phase) and La Niña (the cold phase) of the El Niño Southern Oscillation shows an increased climate variability in the GHA (Fer et al., 2017; Wolff et al., 2011). The major effect of El Niño on drought in the GHA is mainly a decrease in the July–September rainfall in the Ethiopian highlands (Funk et al., 2016; Philip et al., 2018). For instance, the 2015 El Niño phenomenon in Ethiopia was the strongest in decades, and it affected millions of people (Fer et al., 2017; Funk et al., 2016; Philip et al., 2018). Droughts driven by El Niño have affected 19% of the area of Eritrea and Ethiopia, 14–40% of Somalia, and 7–43% of Kenya, while La Niña-driven droughts have affected 7–15% of Sudan, 4–8% of Kenya, 30–60% of Uganda, and 10–38% of Tanzania (Mpelasoka et al., 2018). In addition, climate perturbations in the sea surface temperatures over the Indian Ocean and Pacific Ocean (Fenta et al., 2017), the seasonal migration of the Intertropical Convergence Zone (Liebmann et al., 2014; Tierney et al., 2015), and regional circulations such as the Tropical Easterly Jet, low-level westerlies, localised convergences, monsoons, and Turkana Jet (Nicholson, 2016) have played a role in the increased evolution of drought in the GHA. More specifically, the Indian Ocean sea surface temperatures control the East African rainfall over multi-decadal and longer timescales (Tierney et al., 2013).

Beyond climate variabilities, anthropogenic factors such as deforestation, land-use changes, land degradation, and excessive use and poor management of natural resources have contributed to the occurrence and intensity of drought in the GHA (IPCC, 2013; Lyon, 2014; Trenberth et al., 2014). Therefore, the interacting impacts of climate and human activities on the environment have made drought more frequent, longer, and more intense in

the GHA (Funk et al., 2015; Nicholson, 2017). This suggests that drought monitoring is important to alleviate and mitigate drought events.

#### 4.3. Historical droughts in the Greater Horn of Africa

Providing a comprehensive analysis of historical droughts in the GHA is critical for understanding the underlying characteristics, changing patterns, causes, and implications of drought. Over the last 52 yr, various drought events have been identified spatiotemporally for specific countries and at the GHA level (Table 1). Drought occurrences before the 1990s include the 1973–1974 drought in Ethiopia and the 1984–1985 drought in Ethiopia and Sudan. The former and latter droughts resulted in the deaths of around 250 000 and 450 000 people, respectively (Degefu and Bewket, 2015; Vicente-Serrano et al., 2012). Over the GHA (specifically in the Horn of Africa), drought frequency and duration have increased in the last two decades (Lyon, 2014; Nicholson, 2014) despite differences in drought intensity (Zhan et al., 2016). Prolonged drought events were found during 2000–2001, 2002–2003, 2005–2006, 2008–2009, and 2010–2011 over parts of the GHA (Table 1; AghaKouchak, 2015; Muller, 2014; Nicholson, 2017). However, these droughts presented variations in their severity among the GHA countries, as they did not cover the region with the same magnitude. For instance, during the 2002–2003 drought, about 14 million people were affected in Ethiopia (Funk, 2009), which was the highest in terms of magnitude and distribution for the entire nation. Similarly, the 2008–2009 drought had severe economic consequences as over 13 million people were affected in the GHA (Muller, 2014). The 2010–2011 drought was the worst in 60 yr, and affected over 12 million people in the GHA (AghaKouchak, 2015). The severe 2010–2011 drought affected southeastern GHA countries, including Somalia, Ethiopia, and Kenya. In Somalia alone, about 250 000 deaths were recorded during the 2010–2011 drought (AghaKouchak, 2015; Lyon and Vigaud, 2017). This drought occurred owing to the shortage of October–November rainfall in 2010 and shortage of March–May rainfall in 2011 (Agutu et al., 2017; Anderson et al., 2012).

In addition, all countries in the GHA have experienced severe droughts of different magnitudes. According to the Emergency Events Database (EM-DAT; <http://www.emdat.be/database>), a total of 100 droughts have affected more than 216.9 million people and resulted in 572 thousand deaths and an economic loss of 1.5 million USD in countries in the GHA (Table 1; EM-DAT, 2018; Haile et al., 2019). The spatiotemporal analysis also revealed seven drought episodes during 2002, 2003, 2004, 2005, 2009, 2010, and 2015, which affected large areas of the GHA (Table 1).

Some of the worst droughts in the GHA are shown in Table 1; the occurrence of drought remained largely similar, but with substantial regional differences. Except for Sudan, Djibouti, parts of eastern Ethiopia, eastern Eritrea, and parts of Somalia, drought is becoming recurrent in the GHA. The droughts that occurred in specific GHA countries and the region as a whole are useful for conducting better monitoring and management of drought via informing policy-making and its implementation.

#### 4.4. Droughts and future considerations

Understanding the spatial and temporal patterns of drought events is very important for decision-making. Detecting historical variations of drought occurrences on a seasonal and annual basis is important for implementing drought mitigation measures in the future. In addition, investigation of the key drought parameters at different timescales is fundamental for drought monitoring and management over the GHA. Droughts have increased annually in the GHA, but with substantial regional differences. These varia-

tions were observed in the distribution and magnitude of drought in specific countries or larger areas. This was attributed to natural climate variations and anthropogenic actions. In the GHA, large climate variability can trigger the occurrence of drought (Funk et al., 2015; Nicholson, 2017; Trenberth et al., 2014). In addition, the impacts of human activities on the environment are rarely environmentally friendly and sustainable.

Studies have suggested that the GHA is likely to face more severe and widespread droughts in the future (Masih et al., 2014; Muller, 2014). Increasingly dry conditions are likely due to the intensification of anthropogenic effects, climate variability, and environmental changes. This is pronounced under inefficient drought risk management and weakened power of the stakeholders, governments, and people. The trend of increasing drought will worsen with global warming (IPCC, 2007; Sheffield and Wood, 2008). This suggests that global warming will lead to more land areas being vulnerable to drought (Vicente-Serrano et al., 2013). This would imply an increased desertification process, especially in arid environments under existing climate fluctuations and climate change (Dai, 2011b; IPCC, 2013). Meanwhile, rapid population growth, increasing demand for water, deforestation, land-use changes, and degradation of land and the environment are likely to aggravate the impacts of drought (IPCC, 2007). Thus, holistic and integrated efforts towards drought mitigation are required to minimise the anticipated impacts of droughts in the future. The provision of information and management policies towards drought adaptation and alleviation are required for informing drought policy-making to reduce drought impacts in the GHA.

## 5. Conclusions

In this study, the SPEI was used to analyse the spatiotemporal drought patterns for the period of 1964–2015 in the GHA. The drought characteristic parameters (duration, frequency, and intensity) at monthly, seasonal, and interannual levels were investigated at four timescales (SPEI-01, SPEI-03, SPEI-06, and SPEI-12). Overall, an increasing trend of drought was found for the past 52 yr with distinct spatial and temporal drought patterns. Specifically, the drought increased persistently before the 1990s and became intermittent between 1990 and 2015 with substantial regional variations. The GHA experienced the most serious droughts during 1973–1974, 1984–1985, and 2010–2011, which led to serious damage to societies and the environment. The extent and magnitude of drought tended to increase with the SPEI timescale. The SPEI data from all timescales showed downward trends, thereby indicating that drought has increased in the last five decades. The average trends of changes in the SPEI for the GHA were  $-0.0017 \text{ yr}^{-1}$ ,  $-0.0036 \text{ yr}^{-1}$ ,  $-0.0031 \text{ yr}^{-1}$ , and  $-0.0023 \text{ yr}^{-1}$  for SPEI-01, SPEI-03, SPEI-06, and SPEI-12, respectively, which revealed an increasing trend of drought. The MK trend test and slope indicated that annual drought trends have increased in the GHA. Seasonally, droughts in summer, spring, and winter have increased, but droughts have decreased in the autumn season. This suggested the importance of assessing drought at seasonal and interannual timescales over the GHA. The findings of this study have important implications for creating drought management strategies and adaptation measures. Further efforts should be made towards improving drought prediction skills by considering various climate scenarios under global warming.

## Acknowledgements

Funding for this research was provided by the National Natural Science Foundation of China (Grant Nos. 41730645, 41790424, and 41425002), Strategic Priority Research Program of the Chinese

Academy of Sciences (Grant No. XDA20060402), and International Partnership Program of the Chinese Academy of Sciences (Grant Nos. 131A11KYSB20180034 and 131A11KYSB20170113) and Newton Advanced Fellowship. Data used for this study were obtained from the SPEI dataset (<http://sac.csis.es/spei/database.html>). The first author was sponsored by the Chinese Academy of Sciences-World Academy of Sciences (CAS-TWAS) President's Fellowship Programme for his Ph.D. study at the University of Chinese Academy of Sciences.

## Appendix A. Supplementary data

Supplementary data to this article can be found online at <https://doi.org/10.1016/j.scitotenv.2019.135299>.

## References

- Adhyani, N.L., June, T., Sopaheluwakan, A., 2017. Exposure to drought: duration, severity and intensity (Java, Bali and Nusa Tenggara). *IOP Conf. Ser. Earth Environ. Sci.* 58., <https://doi.org/10.1088/1755-1315/58/1/012040> 012040.
- AghaKouchak, A., 2015. A multivariate approach for persistence-based drought prediction: application to the 2010–2011 East Africa drought. *J. Hydrol.* 526, 127–135. <https://doi.org/10.1016/j.jhydrol.2014.09.063>.
- Agutu, N.O., Awange, J.L., Zerihun, A., Ndehedehe, C.E., Kuhn, M., Fukuda, Y., 2017. Assessing multi-satellite remote sensing, reanalysis, and land surface models' products in characterizing agricultural drought in East Africa. *Remote Sens. Environ.* 194, 287–302. <https://doi.org/10.1016/j.rse.2017.03.041>.
- Allen, R.G., Luis, S.P., RAES, D., Smith, M., 1998. FAO irrigation and drainage Paper No. 56. Crop evapotranspiration (guidelines for computing crop water requirements). *Irrig. Drain.* <https://doi.org/10.1016/j.eja.2010.12.001>.
- Anderson, W.B., Zaitchik, B.F., Hain, C.R., Anderson, M.C., Yilmaz, M.T., Mecikalski, J., Schultz, L., 2012. Towards an integrated soil moisture drought monitor for East Africa. *Hydrol. Earth Syst. Sci.* 16, 2893–2913. <https://doi.org/10.5194/hess-16-2893-2012>.
- Anyah, R.O., Semazzi, F.H.M., 2006. Climate variability over the Greater Horn of Africa based on NCAR AGCM ensemble. *Theor. Appl. Climatol.* 86, 39–62. <https://doi.org/10.1007/s00704-005-0203-7>.
- Asong, Z.E., Wheeler, H.S., Bonsal, B., Razavi, S., Kurkute, S., 2018. Historical drought patterns over Canada and their relation to teleconnections. *Hydrol. Earth Syst. Sci. Discuss.* 1–42. <https://doi.org/10.5194/hess-2018-122>.
- Ayana, E.K., Ceccato, P., Fisher, J.R.B., DeFries, R., 2016. Examining the relationship between environmental factors and conflict in pastoralist areas of East Africa. *Sci. Total Environ.* 557–558, 601–611. <https://doi.org/10.1016/j.scitotenv.2016.03.102>.
- Bachmair, S., Stahl, K., Collins, K., Hannaford, J., Acreman, M., Svoboda, M., Knutson, C., Smith, K.H., Wall, N., Fuchs, B., Crossman, N.D., Overton, I.C., 2016. Drought indicators revisited: the need for a wider consideration of environment and society. *Wiley Interdiscip. Rev. Water* 3, 516–536. <https://doi.org/10.1002/wat2.1154>.
- Baniya, B., Tang, Q., Xu, X., Haile, G.G., Chhipi-Shrestha, G., 2019. Spatial and temporal variation of drought based on satellite derived vegetation condition index in Nepal from 1982–2015. *Sensors (Switzerland)* 19 (430). <https://doi.org/10.3390/s19020430>.
- Brown, M.E., Funk, C.C., 2008. Climate: food security under climate change. *Science* (80-. ). 319, 580–581. <https://doi.org/10.1126/science.1154102>.
- Camberlin, P., 2018. *Climate of Eastern Africa*. Oxford University Press. <https://doi.org/10.1093/acrefore/9780190228620.013.512>.
- Chen, B., Xu, G., Coops, N.C., Ciais, P., Innes, J.L., Wang, G., Myneni, R.B., Wang, T., Krzyzanowski, J., Li, Q., Cao, L., Liu, Y., 2014. Changes in vegetation photosynthetic activity trends across the Asia-Pacific region over the last three decades. *Remote Sens. Environ.* 144, 28–41. <https://doi.org/10.1016/j.rse.2013.12.018>.
- Chen, H., Sun, J., 2015. Changes in drought characteristics over china using the standardized precipitation evapotranspiration index. *J. Clim.* 28, 5430–5447. <https://doi.org/10.1175/JCLI-D-14-00707.1>.
- Dai, A., 2011a. Characteristics and trends in various forms of the palmer drought severity index during 1900–2008. *J. Geophys. Res. Atmos.* 116. <https://doi.org/10.1029/2010JD015541>.
- Dai, A., 2011b. Drought under global warming: a review. *Wiley Interdiscip. Rev. Clim. Chang.* 2, 45–65. <https://doi.org/10.1002/wcc.81>.
- Degefu, M.A., Bewket, W., 2015. Trends and spatial patterns of drought incidence in the Omo-Ghibe River Basin, Ethiopia. *Geogr. Ann. Ser. A Phys. Geogr.* 97, 395–414. <https://doi.org/10.1111/geoa.12080>.
- Dinku, T., Ceccato, P., Connor, S.J., 2011. Challenges of satellite rainfall estimation over mountainous and arid parts of east africa. *Int. J. Remote Sens.* 32, 5965–5979. <https://doi.org/10.1080/01431161.2010.499381>.
- EM-DAT, 2018. Emergency Events Database (EM-DAT) | Centre for Research on the Epidemiology of Disasters [WWW Document], URL <https://www.cred.be/projects/EM-DAT> (accessed 10.21.18).
- Fenta, A.A., Yasuda, H., Shimizu, K., Haregeweyn, N., Kawai, T., Sultan, D., Ebabu, K., Belay, A.S., 2017. Spatial distribution and temporal trends of rainfall and erosivity in the Eastern Africa region. *Hydrol. Process.* 31, 4555–4567. <https://doi.org/10.1002/hyp.11378>.
- Fer, I., Tietjen, B., Jeltsch, F., Wolff, C., 2017. The influence of El Niño-Southern Oscillation regimes on eastern African vegetation and its future implications under the RCP8.5 warming scenario. *Biogeosciences* 14, 4355–4374. <https://doi.org/10.5194/bg-14-4355-2017>.
- Funk, C., 2009. New satellite observations and rainfall forecasts help provide earlier warning of african drought. *Earth Obs.* 21, 23–27.
- Funk, C., Dettinger, M.D., Michaelsen, J.C., Verdin, J.P., Brown, M.E., Barlow, M., Hoell, A., 2008. Warming of the Indian Ocean threatens eastern and southern African food security but could be mitigated by agricultural development. *Proc. Natl. Acad. Sci.* 105, 11081–11086. <https://doi.org/10.1073/pnas.0708196105>.
- Funk, C., Harrison, L., Shukla, S., Hoell, A., Korecha, D., Magadzire, T., Husak, G., Galu, G., 2016. Assessing the contributions of local and East Pacific warming to the 2015 droughts in Ethiopia and Southern Africa [in “Explaining Extremes of 2015 from a Climate Perspective”]. *Bull. Am. Meteorol. Soc.* 96, S75–S80. <https://doi.org/10.1175/BAMS-D-15-00157.1>.
- Funk, C., Nicholson, S.E., Landsfeld, M., Klotter, D., Peterson, P., Harrison, L., 2015. The centennial trends Greater Horn of Africa precipitation dataset. *Sci. Data* 2., <https://doi.org/10.1038/sdata.2015.50> 150050.
- Guha-Sapir, D., Hargitt, D., Hoyois, P., 2004. Thirty years of natural disasters 1974–2003: the numbers.
- Haile, G.G., Tang, Q., Sun, S., Huang, Z., Zhang, X., Liu, X., 2019. Droughts in East Africa: causes, impacts and resilience. *Earth Sci. Rev.* 193, 146–161. <https://doi.org/10.1016/j.earscirev.2019.04.015>.
- Hao, Z., AghaKouchak, A., 2014. A Nonparametric multivariate multi-index drought monitoring framework. *J. Hydrometeorol.* 15, 89–101. <https://doi.org/10.1175/JHM-D-12-0160.1>.
- Harris, I., Jones, P.D., Osborn, T.J., Lister, D.H., 2014. Updated high-resolution grids of monthly climatic observations - the CRU TS3.10 Dataset. *Int. J. Climatol.* 34, 623–642. <https://doi.org/10.1002/joc.3711>.
- IPCC, 2013. *Climate Change 2013: The Physical Science Basis* IPCC Working Group I Contribution to AR5 [WWW Document]. URL <http://www.ipcc.ch/report/ar5/wg1/> (accessed 10.18.18).
- IPCC, 2007. *Climate Change 2007: The Physical Science Basis; Contribution of Working Group I to the Fourth Assessment Report of the Intergovernmental Panel on Climate Change* [WWW Document]. URL [https://www.ipcc.ch/publications\\_and\\_data/publications\\_ipcc\\_fourth\\_assessment\\_report\\_wg1\\_report\\_the\\_physical\\_science\\_basis.htm](https://www.ipcc.ch/publications_and_data/publications_ipcc_fourth_assessment_report_wg1_report_the_physical_science_basis.htm) (accessed 10.21.18).
- He, J., Yang, X., Li, Z., Zhang, X., Tang, Q., 2016. Spatiotemporal variations of meteorological droughts in China during 1961–2014: an investigation based on multi-threshold identification. *Int. J. Disaster Risk Sci.* 7, 63–76. <https://doi.org/10.1007/s13753-016-0083-8>.
- Kendall, M.G., 1955. *Rank correlation methods*. Oxford, England.
- Lee, S.H., Yoo, S.H., Choi, J.Y., Bae, S., 2017. Assessment of the impact of climate change on drought characteristics in the Hwanghae Plain, North Korea using time series SPI and SPEI: 1981–2100. *Water (Switzerland)* 9. <https://doi.org/10.3390/w9080579>.
- Liebmann, B., Hoerling, M.P., Funk, C., Bladé, I., Dole, R.M., Allured, D., Quan, X., Pegion, P., Eischeid, J.K., 2014. Understanding recent eastern Horn of Africa rainfall variability and change. *J. Clim.* 27, 8630–8645. <https://doi.org/10.1175/JCLI-D-13-00714.1>.
- Liu, Z., Wang, Y., Shao, M., Jia, X., Li, X., 2016. Spatiotemporal analysis of multiscalar drought characteristics across the Loess Plateau of China. *J. Hydrol.* 534, 281–299. <https://doi.org/10.1016/j.jhydrol.2016.01.003>.
- López-Moreno, J.L., Vicente-Serrano, S.M., Zabalza, J., Beguería, S., Lorenzo-Lacruz, J., Azorin-Molina, C., Morán-Tejeda, E., 2013. Hydrological response to climate variability at different time scales: a study in the Ebro basin. *J. Hydrol.* 477, 175–188. <https://doi.org/10.1016/j.jhydrol.2012.11.028>.
- Lyon, B., 2014. Seasonal drought in the Greater Horn of Africa and its recent increase during the March-May long rains. *J. Clim.* 27, 7953–7975. <https://doi.org/10.1175/JCLI-D-13-00459.1>.
- Lyon, B., Dewitt, D.G., 2012. A recent and abrupt decline in the East African long rains. *Geophys. Res. Lett.* 39, 1–5. <https://doi.org/10.1029/2011GL050337>.
- Lyon, B., Vigaud, N., 2017. Unraveling East Africa's climate paradox climate extremes: patterns and mechanisms. *Geophys. Monogr.* 226. <https://doi.org/10.1002/9781119068020.ch16>.
- Mann, H.B., 1945. Nonparametric tests against trend. *Econometrica* 13, 245. <https://doi.org/10.2307/1907187>.
- Mao, Y., Wu, Z., He, H., Lu, G., Xu, H., Lin, Q., 2017. Spatio-temporal analysis of drought in a typical plain region based on the soil moisture anomaly percentage index. *Sci. Total Environ.* 576, 752–765. <https://doi.org/10.1016/j.scitotenv.2016.10.116>.
- Masih, I., Maskey, S., Mussá, F.E.F., Trambauer, P., 2014. A review of droughts on the African continent: a geospatial and long-term perspective. *Hydrol. Earth Syst. Sci.* 18, 3635–3649. <https://doi.org/10.5194/hess-18-3635-2014>.
- McKee, T.B., Doesken, N.J., Kleist, J., 1993. The relationship of drought frequency and duration to time scales, Eighth Conference on Applied Climatology.
- Measho, S., Chen, B., Trisurat, Y., Pellikka, P., Guo, L., Arunyawat, S., Tuankrwa, V., Ogbazghi, W., Yemane, T., 2019. Spatio-temporal analysis of vegetation dynamics as a response to climate variability and drought patterns in the Semiarid Region, Eritrea. *Remote Sens.* 11, 724. <https://doi.org/10.3390/rs11060724>.

- Mishra, A.K., Singh, V.P., 2010. A review of drought concepts. *J. Hydrol.* 391, 202–216. <https://doi.org/10.1016/j.jhydrol.2010.07.012>.
- Mpelasoka, F., Awange, J.L., Zerihun, A., 2018. Influence of coupled ocean-atmosphere phenomena on the Greater Horn of Africa droughts and their implications. *Sci. Total Environ.* 610–611, 691–702. <https://doi.org/10.1016/j.scitotenv.2017.08.109>.
- Mukherjee, S., Mishra, A., Trenberth, K.E., 2018. Climate change and drought : a perspective on drought indices climate change and drought : a perspective on drought indices. doi:10.1007/s40641-018-0098-x
- Muller, J.C.Y., 2014. Adapting to climate change and addressing drought - learning from the Red Cross Red Crescent experiences in the Horn of Africa. *Weather Clim. Extrem.* 3, 31–36. <https://doi.org/10.1016/j.wace.2014.03.009>.
- New, M., Hulme, M., Jones, P., 2000. Representing twentieth-century space-time climate variability. Part II: development of 1901–96 monthly grids of terrestrial surface climate. *J. Clim.* 13, 2217–2238.
- Nicholson, S., 2016. The Turkana low-level jet: mean climatology and association with regional aridity. *Int. J. Climatol.* 36, 2598–2614. <https://doi.org/10.1002/joc.4515>.
- Nicholson, S.E., 2017. Climate and climatic variability of rainfall over eastern Africa. *Rev. Geophys.* 55, 590–635. <https://doi.org/10.1002/2016rg000544>.
- Nicholson, S.E., 2014. A detailed look at the recent drought situation in the Greater Horn of Africa. *J. Arid Environ.* 103, 71–79. <https://doi.org/10.1016/j.jaridenv.2013.12.003>.
- Ntale, H.K., Gan, T.Y., 2003. Drought indices and their application to East Africa. *Int. J. Climatol.* 23, 1335–1357. <https://doi.org/10.1002/joc.931>.
- Ogallo, L., Bessemoulin, P., Ceron, J.-P., Mason, S., Connor, S.J., 2008. Adapting to climate variability and change: the Climate Outlook Forum process. *WMO Bull.* 57, 93–101.
- Palmer, 1965. Meteorological drought. Research Paper No. 45, Department of Commerce, Washington D.C., D 58 pp.
- Philip, S., Kew, S.F., van Oldenborgh, G.J., Otto, F., O'Keefe, S., Hausteine, K., King, A., Zegeye, A., Eshetu, Z., Hailemariam, K., Singh, R., Jjemba, E., Funk, C., Cullen, H., 2018. Attribution analysis of the Ethiopian drought of 2015. *J. Clim.* 31, 2465–2486. <https://doi.org/10.1175/JCLI-D-17-0274.1>.
- Potopová, V., Štěpánek, P., Zahradníček, P., Farda, A., Türkott, L., Soukup, J., 2018. Projected changes in the evolution of drought on various timescales over the Czech Republic according to Euro-CORDEX models. *Int. J. Climatol.* 38, e939–e954. <https://doi.org/10.1002/joc.5421>.
- Rhee, J., Cho, J., 2015. Future changes in drought characteristics: regional analysis for South Korea under CMIP5 projections. *J. Hydrometeorol.* 17, 437–451. <https://doi.org/10.1175/jhm-d-15-0027.1>.
- Schreck, C.J., Semazzi, F.H.M., 2004. Variability of the recent climate of eastern Africa. *Int. J. Climatol.* 24, 681–701. <https://doi.org/10.1002/joc.1019>.
- Schwalm, C.R., Anderegg, W.R.L., Michalak, A.M., Fisher, J.B., Biondi, F., Koch, G., Litvak, M., Ogle, K., Shaw, J.D., Wolf, A., Huntzinger, D.N., Schaefer, K., Cook, R., 2017. Letter. *Nat. Publ. Gr.* 548, 202–205. <https://doi.org/10.1038/nature23021>.
- Sheffield, J., Wood, E.F., 2008. Projected changes in drought occurrence under future global warming from multi-model, multi-scenario, IPCC AR4 simulations. *Clim. Dyn.* 31, 79–105. <https://doi.org/10.1007/s00382-007-0340-z>.
- Sheffield, J., Wood, E.F., Roderick, M.L., 2012. Little change in global drought over the past 60 years. *Nature* 491, 435–438. <https://doi.org/10.1038/nature11575>.
- Sivakumar, M.V.K., Stefanski, R., Bazza, M., Zelaya, S., Wilhite, D., Magalhaes, A.R., 2014. High level meeting on national drought policy: summary and major outcomes. *Weather Clim. Extrem.* 3, 126–132. <https://doi.org/10.1016/j.wace.2014.03.007>.
- Spinoni, J., Naumann, G., Carrao, H., Barbosa, P., Vogt, J., 2014. World drought frequency, duration, and severity for 1951–2010. *Int. J. Climatol.* 34, 2792–2804. <https://doi.org/10.1002/joc.3875>.
- Steinemann, A., Iacobellis, S.F., Cayan, D.R., 2015. Developing and Evaluating Drought Indicators for Decision-Making. *J. Hydrometeorol.* 16, 1793–1803. <https://doi.org/10.1175/jhm-d-14-0234.1>.
- Tadesse, T., Senay, G., Wardlow, B.D., Knutson, C.L., Haile, M., 2008. The need for integration of drought monitoring tools for proactive food security management in Sub-Saharan Africa food security management in sub-Saharan Africa. *Nat. Resour. Forum* 32, 265–279.
- Tierney, J.E., Smerdon, J.E., Anchukaitis, K.J., Seager, R., 2013. Multidecadal variability in East African hydroclimate controlled by the Indian Ocean. *Nature* 493, 389–392. <https://doi.org/10.1038/nature11785>.
- Tierney, J.E., Ummerhofer, C.C., DeMenocal, P.B., 2015. Supplementary materials for: past and future rainfall in the Horn of Africa. *Sci. Adv.* 1, <https://doi.org/10.1126/sciadv.1500682> e1500682.
- Trenberth, K.E., Dai, A., Van Der Schrier, G., Jones, P.D., Barichivich, J., Briffa, K.R., Sheffield, J., 2014. Global warming and changes in drought. *Nat. Clim. Chang.* 4, 17–22. <https://doi.org/10.1038/nclimate2067>.
- UNDP/UNSO, 1997. Aridity zones and dryland populations: an assessment of population levels in the world's drylands with particular reference to Africa. UNDP Office to Combat Desertification and Drought (UNSO), New York.
- United Nations, 2014. Land and drought | UNCCD, New York, USA [WWW Document]. URL <https://www.unccd.int/issues/land-and-drought> (accessed 10.18.18)
- Van Loon, A.F., 2015. Hydrological drought explained. *Wiley Interdiscip. Rev. Water* 2, 359–392. <https://doi.org/10.1002/wat2.1085>.
- Vicente-Serrano, S.M., Beguería, S., Gimeno, L., Eklundh, L., Giuliani, G., Weston, D., El Kenawy, A., López-Moreno, J.L., Nieto, R., Ayenew, T., Konte, D., Ardö, J., Pegram, G.G.S., 2012. Challenges for drought mitigation in Africa: the potential use of geospatial data and drought information systems. *Appl. Geogr.* 34, 471–486. <https://doi.org/10.1016/j.apgeog.2012.02.001>.
- Vicente-Serrano, Sergio M., Beguería, S., López-Moreno, J.L., 2010a. A multiscale drought index sensitive to global warming: the standardized precipitation evapotranspiration index. *J. Clim.* 23, 1696–1718. <https://doi.org/10.1175/2009JCLI2909.1>.
- Vicente-Serrano, S.M., Beguería, S., López-Moreno, J.L., Angulo, M., El Kenawy, A., 2010b. A new global 0.5° Gridded Dataset (1901–2006) of a multiscale drought index: comparison with current drought index datasets based on the palmer drought severity index. *J. Hydrometeorol.* 11, 1033–1043. <https://doi.org/10.1175/2010JHM1224.1>.
- Vicente-Serrano, S.M., Gouveia, C., Camarero, J.J., Beguería, S., Trigo, R., Lopez-Moreno, J.L., Azorin-Molina, C., Pasho, E., Lorenzo-Lacruce, J., Revuelto, J., Moran-Tejeda, E., Sanchez-Lorenzo, A., 2013. Response of vegetation to drought timescales across global land biomes. *Proc. Natl. Acad. Sci.* 110, 52–57. <https://doi.org/10.1073/pnas.1207068110>.
- Wang, F., Wang, Z., Yang, H., Zhao, Y., 2018. Study of the temporal and spatial patterns of drought in the Yellow River basin based on SPEI. *Sci. China Earth Sci.* 61, 1098–1111. <https://doi.org/10.1007/s11430-017-9198-2>.
- Wolff, C., Haug, G., Timmermann, A., 2011. Reduced interannual rainfall variability in East Africa during reduced interannual rainfall variability in East Africa during the last ice age variability in East Africa during the last ice age. *Nature* 133, 743–748.
- Xu, K., Yang, D., Yang, H., Li, Z., Qin, Y., Shen, Y., 2015. Spatio-temporal variation of drought in China during 1961–2012: a climatic perspective. *J. Hydrol.* 526, 253–264. <https://doi.org/10.1016/j.jhydrol.2014.09.047>.
- Xu, L., Chen, N., Zhang, X., 2018. Global drought trends under 1.5 and 2 C warming. *Int. J. Climatol.* 1–11. <https://doi.org/10.1002/joc.5958>.
- Yevjevich, V., 1967. An objective approach to definitions and investigations of continental hydrologic drought s an objective approach to definitions and investigations of continental hydrologic droughts. Hydrology papers, Colorado state university. Fort Collins, Colorado.
- Yu, M., Li, Q., Hayes, M.J., Svoboda, M.D., Heim, R.R., 2014. Are droughts becoming more frequent or severe in China based on the standardized precipitation evapotranspiration index: 1951–2010? *Int. J. Climatol.* 34, 545–558. <https://doi.org/10.1002/joc.3701>.
- Zhan, W., Guan, K., Sheffield, J., Wood, E.F., 2016. Depiction of drought over sub-Saharan Africa using reanalyses precipitation data sets. *J. Geophys. Res. Atmos.* 121, 10555–10574. <https://doi.org/10.1002/2016JD024858>.
- Zhang, Q., Qi, T., Singh, V.P., Chen, Y.D., Xiao, M., 2015. Regional frequency analysis of droughts in China: a multivariate perspective. *Water Resour. Manag.* 29, 1767–1787. <https://doi.org/10.1007/s11269-014-0910-x>.
- Zhou, L., Wu, J., Mo, X., Zhou, H., Diao, C., Wang, Q., Chen, Y., Zhang, F., 2017. Quantitative and detailed spatiotemporal patterns of drought in China during 2001–2013. *Sci. Total Environ.* 589, 136–145. <https://doi.org/10.1016/j.scitotenv.2017.02.202>.